Preprints (www.preprints.org) | NOT PEER-REVIEWED | Posted: 6 July 2021 doi:10.20944/preprints202107.0128.v1

Characterization and Thermal Aging Tests of Cr Based Multilayer for Unconcentrated Solar Thermal Applications

Antonio CALDARELLI[1,2], Carmine D'ALESSANDRO[1,2], Davide DE MAIO[1,2], Daniela DE LUCA[2,3], Eliana GAUDINO[1,2], Marilena MUSTO[1], Emiliano DI GENNARO[3] and Roberto RUSSO[2]

[1] Industrial Engineering Department, University of Napoli "Federico II", Napoli, Italy
[2] Institute of Applied Sciences and Intelligent Systems, National Research Council of Italy, Napoli Unit, Italy
[3] Physics Department, University of Napoli "Federico II", Napoli, Italy
Corresponding author e-mail: antonio.caldarelli@na.isasi.cnr.it, antonio.caldarelli@unina.it

Abstract

Optical characterization and thermal aging tests are performed on a sputter-deposited coating, consisting of $SiO_2/Cr_2O_3/Cr/Cr_2O_3$ layers, designed and developed as a selective solar absorber to be used for unconcentrated solar thermal applications. Both measurements are performed by using a home-made apparatus, which mimics a flat plate collector under high vacuum. A Performance Criterion ($PC_\eta(T)$), based on absorber efficiency is proposed, and a forecast of service lifetime is obtained. As a result of the thermal aging tests, the selective solar absorber under study appears to be highly efficient at mid temperatures (up to 573 K) and thermally stable at temperatures (up to 690 K).

Keywords: Spectrally selective coating; Optical properties; Thermal stability; High temperature emissivity; Energy activation; Prediction of lifetime test; Thermal aging.

1. Introduction

Global warming and energy crisis have increasingly led to the use of renewable energies. Wind power [1], hydropower [2], solar energy [3], geothermal energy [4] and bio energy [5] are commonly used for generation of electricity and heating & cooling. Solar energy is inexhaustible and abundant, the most popular routes for harvesting solar energy are photovoltaics [3] and thermal process [6]. In particular, solar thermal energy can be used to satisfy Heating and Cooling demand that represents about one third of world energy consumption. Solar collectors produce thermal energy converting sunlight into heat. They can be classified into two categories: non-concentrating [7] and concentrating [8]. Flat plate collectors are non-concentrating type collectors that are mainly used for hot water production and in industrial process heat applications. TVPSolar developed a flat plate collectors using ultra high-vacuum technology [9]. Thanks to high-vacuum insulation, convective losses are reduced to negligible level and the collector can work in mid-temperature regime (up to 473 K). The main component for improving the energy efficiency in high vacuum solar collectors is the selective absorber. It converts the incident solar radiation into heat minimizing heat losses due to radiation emission. The Selective Solar Absorber (SSA) performances are defined by the solar absorptance and the thermal emittance. The Kirchhoff's law of thermal radiation states that, for a given surface the absorptivity $\alpha(\lambda)$ must be equal to emissivity $\varepsilon(\lambda)$. In samples with zero transmissivity (for opaque material) the energy conservation implies that the reflectivity is the complement of absorptivity (eq.1):

$$\alpha(\lambda) = \varepsilon(\lambda) = 1 - T(\lambda) - R(\lambda) = 1 - R(\lambda) \quad (1)$$

According to the standard ISO 22975, the solar absorptance (α_s) can be defined as the ratio of the total absorbed solar energy and the incident solar flux H_{abs} as reported in the eq.2:

$$\alpha_s = \frac{\int_{0.3\mu m}^{2.5\mu m} \alpha(\lambda) S(\lambda) d\lambda}{\int_{0.3\mu m}^{2.5\mu m} S(\lambda) d\lambda} \quad (2)$$

with $S(\lambda)$ the solar radiation on the absorber and the spectral averaged thermal emissivity ($\bar{\varepsilon}(T)$) can be defined as eq.3:

Preprints (www.preprints.org) | NOT PEER-REVIEWED | Posted: 6 July 2021 doi:10.20944/preprints202107.0128.v1

$$\bar{\varepsilon}(T) = \frac{\int_0^\infty \varepsilon_\lambda(\lambda) E_{BB}(\lambda,T)\,d\lambda}{\int_0^\infty E_{BB}(\lambda,T)\,d\lambda} \quad (3)$$

with $E_{BB}(\lambda, T)$ is the temperature dependent blackbody spectral emission given by Planck's formula.

Solar energy is mainly concentrated in the spectral range 0.3–2.5 μm, instead thermal emission at mid temperatures occurs at wavelengths longer than 2 μm. Hence, the ideal SSA should absorb all the solar radiation ($\alpha(\lambda) = 1$) up to a given wavelength and reflects all the thermal radiation ($\varepsilon(\lambda) = 0$) above the same wavelength. In figure 1, the emissivity curve of an ideal absorber is reported and the transition wavelength is defined according to energetic consideration [10]. To obtain the desired selectivity, the solar absorbers are often realized using the thin film technology.

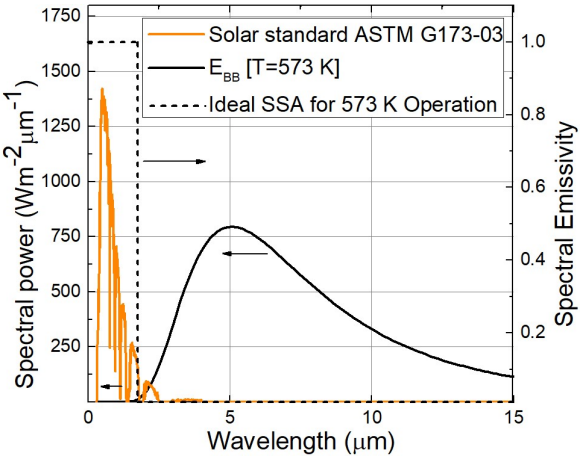

FIGURE 1. Ideal absorber spectral emissivity designed for 573 K (black dashed line), blackbody emission E_{BB} at 573 K (black line) and Solar Spectrum (orange line).

The absorber efficiency ($\eta_{abs}(T)$) is usually defined as eq.4:

$$\eta_{abs}(T) = \frac{q_h}{H_{abs}} = \alpha_s - \bar{\varepsilon}\frac{\sigma(T_a^4 - T_{amb}^4)}{H_{abs}} \quad (4)$$

where q_h is the absorbed power, H_{abs} is the heat flux incident on the thermal system, σ is the Stefan–Boltzmann constant, T_a is the absorber temperature, T_{amb} is the ambient temperature. The negative term in eq. 4 is responsible for the system efficiency reduction and it defines the main source of thermal loss [10].

Solar absorptance and spectral averaged thermal emissivity are usually evaluated by measuring spectral reflectivity with an optical spectrophotometer and a Fourier Transform Infrared spectrophotometer [11], [12] at room temperature, neglecting its temperature dependence.

In this work, the absorptance (α_s) and spectral averaged emissivity ($\bar{\varepsilon}(T)$) of a recently developed SSA [13] at its working temperature were estimated, by means of the Mini Test Box (MTB) system [13, 14]. It is an home-made calorimetric emissometer which reproduces a flat plate collector under high vacuum conditions and equipped with a calibrated LED array system [15] as artificial light source. According to Eq. (2) since most absorber have very high values of absorptivity up to 2 μm the solar absorptances calculated using the SUN Spectrum and the LED spectrum differ only few per cent [16].With the same apparatus thermal aging tests for the aforementioned SSA were also carried out to study degradation time of the coating, due to the high operating temperature. In respect to the typically used ovens for such purpose, our system presents a clear advantage: it allows for a real time monitoring of the changes of optical properties during the thermal aging test.

2. Performance Criterion Definition

Absorber optical properties are measured and optimized during development process at room temperature, but these properties may vary with the operating temperature and can change during the operation time. For this reason, it is advisable to evaluate the optical properties of the absorber at working temperature and predict

Preprints (www.preprints.org) | NOT PEER-REVIEWED | Posted: 6 July 2021 doi:10.20944/preprints202107.0128.v1

the aging behaviour of these coatings. The International Energy Agency (IEA) formulated an accelerated thermal stability testing and service life predication method for solar absorber coatings [17]. This method is currently the standard named ISO/CD 12592, 2 "Solar Energy – Materials for flat-plate collectors – Qualification test procedures for solar surface durability" [17]. Such standard, being developed for standard collector working in air at low temperature, is not adequate to evaluate the service lifetime of solar absorber in evacuated flat collectors, however it represents a useful starting point for this study. The standard assumes that the degradation is caused by diffusion processes according to the Arrhenius' law:

$$k = D_{Arrh}\, exp\left(-\frac{E_T}{R\,T}\right) \tag{5}$$

where k is the chemical reaction rate, D_{Arrh} is the Arrhenius constant, R is the constant of ideal gas, T is the temperature, and E_T is the activation energy per mole of the ageing process according to Arrhenius' law, which is the fundamental coating parameter that determines the ageing resistance at the operating temperature.

The exponential temperature dependence of the Arrhenius law allows to perform accelerated aging tests using a temperature higher than the operating temperature and to estimate the failure time (the time at which the absorber efficiency is reduced more than the value defined according to the reported standard). However, the absorber temperature changes during the normal working conditions. Such temperature variations can be summarized by a temperature frequency function $f(T)$ that represents how many hours the absorber is at temperature T during one-year operation. According to the Arrhenius law, it is possible to replace the function $f(T)$ (that have a complex shape) with an effective constant temperature T_{eff} that produces the same aging effect than the real $f(T)$:

$$exp\left(-\frac{E_T}{R}T_{eff}^{-1}\right) = \int_{T_{min}}^{T_{max}} exp\left(-\frac{E_T}{R}T^{-1}\right) f(T)dT \tag{6}$$

where T_{max} and T_{min} are the maximum and minimum temperature of the solar absorber observed over one year operation and $f(T)$ is the temperature frequency function. The standard [17] defines $f(T)$ for Domestic Hot Water (DHW) applications. It is obtained as the averaged measured values from four different flat-plate collectors, exposed for one year in Rapperswil (Switzerland). The panels were kept for 11 months in operation and for 30 days at stagnation.

Once the T_{eff} is calculated, and if the activation energy E_T is known, it is possible to calculate a failure time (t_R in years) corresponding to a testing temperature (T_R). For a coating with an expected service lifetime of 25 years the t_R value can be determined by:

$$t_R = 25 \exp\left[-\frac{E_T}{R}\left(\frac{1}{T_{eff}} - \frac{1}{T_R}\right)\right] \tag{7}$$

The values of t_R and T_R are a compromise between the requirements of a testing time easily accessible (no more than few weeks), easily measurable with a small relative error (at least one hours), and a testing temperature not too higher than the stagnation temperature, to avoid the activation of other degradation mechanisms (with a different activation energy).

To estimate the activation energy, the standard procedure aims to obtain the same degradation in two tests performed at different temperatures. According to IEA [17], the degree of aging of a coating can be evaluated through the product of the chemical reaction rate (k) and the time of the chemical reaction (t), called Performance Criterion (PC); it can be also evaluated by measuring the optical characteristics of the absorber:

$$PC = k \cdot t = -\Delta\alpha + 0.5\Delta\bar{\varepsilon} \tag{8}$$

where $\Delta\alpha = \alpha_S' - \alpha_S$, $\Delta\bar{\varepsilon} = \bar{\varepsilon}_t' - \bar{\varepsilon}_t$, α_S' ($\bar{\varepsilon}_t'$) represents the absorptance (the emittance) after testing, and α_S ($\bar{\varepsilon}_t$) the absorptance (the emittance) of the virgin sample. The different roles and weights of absorptance and emittance in determine the efficiency in the solar thermal collector for DHW applications define the signs and the factor 0.5 in eq.8. As a consequence, an operating temperature higher than 373 K would require adjusting the weighting factor of $\Delta\varepsilon$ in eq. 8 according to the temperature.

Preprints (www.preprints.org) | NOT PEER-REVIEWED | Posted: 6 July 2021 doi:10.20944/preprints202107.0128.v1

The PC value is periodically measured during the tests, and the ageing test is stopped when a measurement returns a PC value higher than 0.05, which has been defined as the maximum degradation for a service lifetime of 25 years (Standard ISO/CD 12592, 2). The time when the PC reaches 0.05 during testing is not experimentally accessible and it is usually extrapolated from the different measurements. Such extrapolated time value can be used in eq. 7 to evaluate the service lifetime.

Furthermore, by writing eq.5 for two different test temperatures T_1 and T_2 and multiplying both members by the testing times t_1 and t_2, D_{Arr} and E_T can be calculated:

$$k_1 t_1 = t_1 D_{Arr} \exp\left(-\frac{E_T}{RT_1}\right) \quad (9.a)$$

$$k_2 t_2 = t_2 D_{Arrh} \exp\left(-\frac{E_T}{RT_2}\right) \quad (9.b)$$

where the first term of both equations (9.a and 9.b) is PC.

The knowledge of E_T and D_{Arr} allows to use Eq. 9 to calculate the service lifetime (t), for a specific PC, under the working conditions imposed by T without the need of extrapolating the time value as it is the case in eq. 7.

3. Experimental details

The SSA under test consists of 4 layers deposited by sputtering on a copper substrate [18] from the top to the bottom $SiO_2/Cr_2O_3/Cr/Cr_2O_3$. The total thickness of the multilayer is about 150 nm, and the single layer thicknesses were obtained to maximize the absorber efficiency at 1000 W/m^2 and 573 K operating temperature as reported in [18]. The characterization and the ageing test were performed in the MTB system [13, 14]. It consists of a stainless-steel vessel closed on its upper side by an extra-clear glass where the absorber is suspended by supports of negligible thermal conductivity. The vacuum is obtained by a turbomolecular pump that keeps the pressure below 10^{-2} Pa to reduce to a negligible level both convective and conductive losses of internal gas. A LED array system [15], consisting in 4 identical LED arrays is used as a controlled source of heating (fig.2).

The radiative properties of the SSA are determined through a calorimetric approach; the power balance equation of the absorber under vacuum is:

$$m_a\, c_p(T_a) \frac{d\,T_a}{dt} = \alpha_L\, A\, \tau\, P_{in} - \bar{\varepsilon}_a(T_a)\, \sigma\, A \left(T_a^4 - T_g^4\right) - \bar{\varepsilon}_{sub}(T_{sub})\, \sigma\, A \left(T_a^4 - T_v^4\right) \quad (10)$$

where m_a, c_p, T_a, α_L, A are mass, specific heat capacity, temperature, absorptance and area of the absorber under test respectively; τ is the glass transmittance, P_{in} is the incident light power per unit of area, $\bar{\varepsilon}_a(T_a)$ is the SSA thermal emittance defined according to eq.3, T_g is the glass temperature, $\bar{\varepsilon}_{sub}(T_{sub})$ is the substrate thermal emittance and T_v is the vessel temperature.

Preprints (www.preprints.org) | NOT PEER-REVIEWED | Posted: 6 July 2021 doi:10.20944/preprints202107.0128.v1

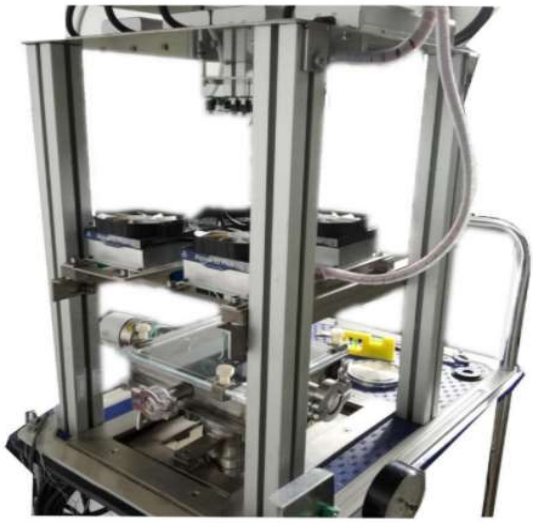

FIGURE 2. The mini test box system with LED array system.

It is worth to note that all temperatures are expressed in kelvin and α_L is calculate according to eq.2, where the Sun spectrum $S(\lambda)$ is replaced by the LED spectrum $S_L(\lambda)$. It has been experimentally verified that, during measurement, T_g and T_v differ by few degrees and the eq.10 can be rewritten as:

$$m_a\, c_p(T_a) \frac{d\, T_a}{dt} = \alpha_L\, A\, \tau\, P_{in} - \bar{\varepsilon}_{tot}(T_a)\, \sigma\, A\, (T_a^4 - T_m^4) \qquad (11)$$

where $\bar{\varepsilon}_{tot}(T_a)$ is the sum between $\bar{\varepsilon}_a(T_a)$ and $\bar{\varepsilon}_{sub}(T_{sub})$ and T_m is the average between T_g and T_v. All values in eq.11 are experimentally accessible and can be measured with high precision except the absorptance α_L and the thermal emittance $\bar{\varepsilon}_{tot}(T_a)$. During a cooling down phase ($P_{in} = 0$), $\bar{\varepsilon}_{tot}(T_a)$ is the only unknown quantity and can be calculated, and the results for the sample under test are reported in figure 3a.

Once the thermal emittance is known, the absorptance (α_L) can be calculated from the heating up phase. The α_L value was also calculated according to eq.2, measuring the hemispherical reflectivity with integrating sphere and an Optical Spectrum Analyser at room temperature. The absorptivity curve obtained by reflectivity measurements is reported in figure 3b (blue line) with the LED Spectrum (red line). The spectrally averaged absorptivity (α_{Lo}) is equal to 0.979 whereas the MTB measurement (α_L) returned a value of 0.965 in agreement with the previous independent measurement.

The fitting procedure of thermal emittance is limited to 373 K since, below this value, the temperature variations $\left(\frac{dT_a}{dt}\right)$ are very small over time and emissivity values are constant within the experimental error.

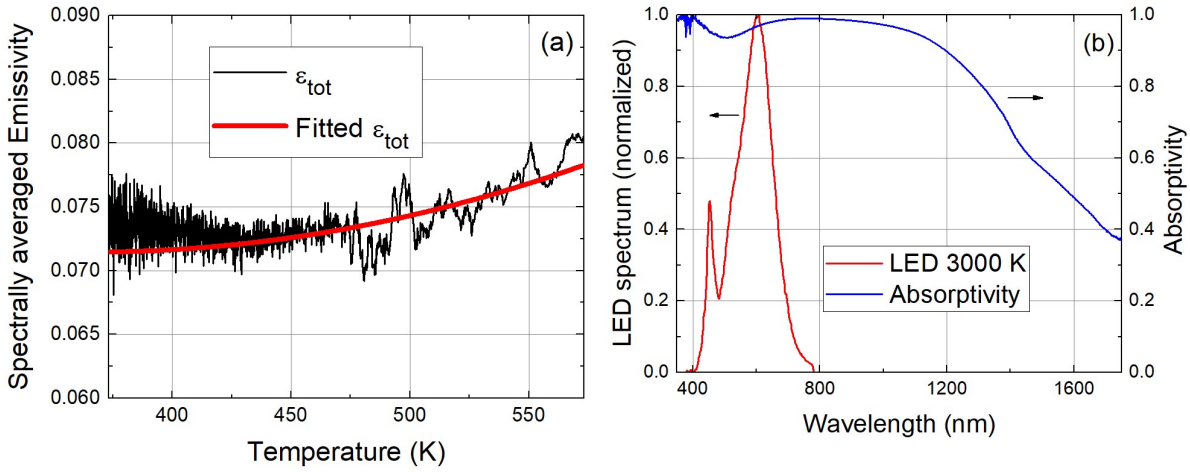

Preprints (www.preprints.org) | NOT PEER-REVIEWED | Posted: 6 July 2021 doi:10.20944/preprints202107.0128.v1

FIGURE 3. a) Spectral averaged emissivity ($\bar{\varepsilon}_{tot}(T_a)$) calculated by means MTB system (black line) and fitted (red line) b) Left axis: spectrum on the LED Array used to illuminate the absorber. Right axis: absorptivity measured with integrating sphere and an Optical spectrum analyser at room temperature.

To determine the value of $\bar{\varepsilon}_a(T_a)$ it is necessary to subtract $\bar{\varepsilon}_{sub}(T_{sub})$ from $\bar{\varepsilon}_{tot}(T_a)$. A copper bulk substrate was used to measure the substrate thermal emittance with MTB system and the results are reported in fig.4a. In this measurement the thermal emittance refers to the copper bulk substrate having the two surfaces with the same properties; $\bar{\varepsilon}_{sub}(T_{sub})$ from a single substrate surface can be obtained by dividing the experimental data plotted in fig.4a by a factor two. Such values have to be subtracted to $\bar{\varepsilon}_{tot}(T_a)$ to obtain the spectral averaged emissivity $\bar{\varepsilon}_a(T_a)$ of the solar selective absorber under test and the results are reported in figure 4b.

The SSA under test presents a high absorption (0.965) and a low emissivity (0.057) at operating temperature (573 K). The low emissivity value is crucial for absorber working in mid-high temperature range [10], for this reason this SSA is very efficient for mid-high temperature applications. The efficiency value $\eta_{abs}(T)$ at T_a = 573 K is 0.640 (calculated according to eq.4 with T_{amb} = 293 K and H_{abs} = 1000 W/m^2).

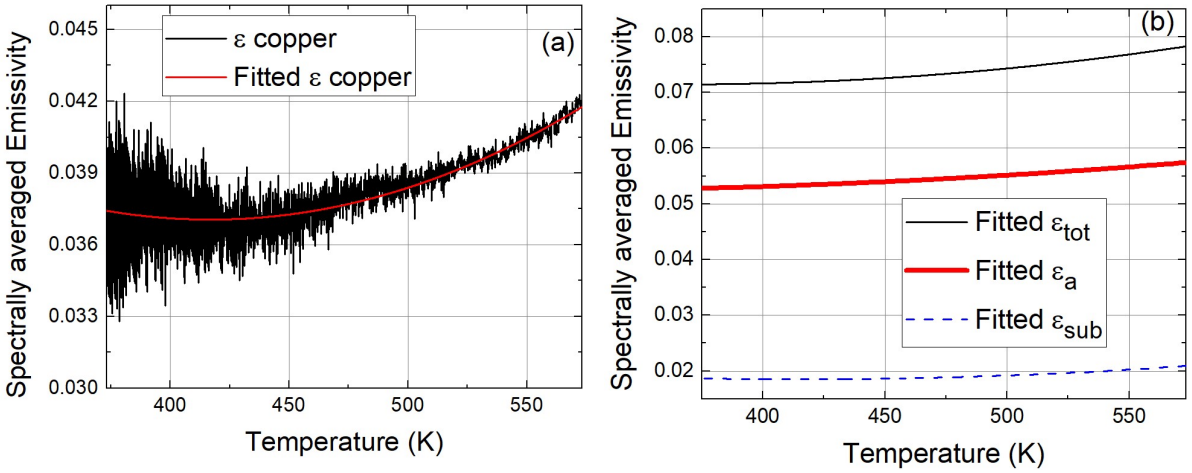

FIGURE 4. (a) Spectral averaged emissivity calculated by means MTB system for copper (black line) and fitted (red line). (b) The thermal emittance as function of temperature of: the whole sample ($\bar{\varepsilon}_{tot}(T_a)$ black line), the copper substrate ($\bar{\varepsilon}_{sub}(T_{sub})$ blue dashed line), and the SSA under test ($\bar{\varepsilon}_a(T_a)$ thick red line).

4. Results and Discussion

During the service lifetime of a SSA, due to the operating temperature, optical properties can change leading to an unacceptable loss of efficiency. To study this degradation two aging thermal tests were carried out on the solar selective absorber by means MTB system. One of the main advantages of using the MTB system is the possibility to perform real time optical measurements on the absorber, while it remains in high-vacuum condition.

During the first test, the absorber was kept at 673 K for a total time of 262 hours. Several measurements of the optical characteristics were performed during the testing time without breaking the vacuum (see fig. 5). The absorber temperature was kept constant adjusting the incident power to satisfy the eq.11 in equilibrium conditions: $\alpha_L\, A\, \tau\, P_{in} = \bar{\varepsilon}_{tot}(T_a)\, \sigma\, A\, (T_a^4 - T_m^4)$.

The changes in the optical characteristics describe the coatings aging degree. In fig.5a is shown the decreasing trend in absorptance, during the first test, from an initial value equal to 0.967 up to reach a value of 0.885 after 262 hours at a temperature of 673 K, with a decrease by 8.5% absorptance. The decrease in absorptance is probably due to interdiffusion phenomena within the coating.

Optical measurements of absorptance, made before and after the ageing test, show agreement with the calorimetric ones, as shown in fig. 5a. A similar, but less pronounced, behaviour has been observed for the spectral averaged emissivity at 573 K (see fig.5b), which registers a decreasing of 7.7% after 87 hours at a temperature of 673 K, from an initial value of 0.057 to a final value of 0.052. After 87 hours the spectral

Preprints (www.preprints.org) | NOT PEER-REVIEWED | Posted: 6 July 2021 doi:10.20944/preprints202107.0128.v1

averaged emissivity at 573 K increases slightly and assumes a value of 0.055 after 262 hours. The difference between the values of spectral averaged emissivity before and after performing the aging test is very small, only 2.5%, showing a good stability under vacuum conditions of the SSA at 673 K.

To calculate E_T and D_{Arrh} through eq.9, it is necessary to know $PC = k \cdot t$. For standard ISO/CD 12592, 2 the PC is a combination of optical properties (eq.8), but the standard test was based on load profiles for absorbers used for DHW system, in which, due to the low operating temperature the weight of emittance is one half of absorptance. For mid-high temperature applications, the relative importance of the absorber thermal emittance respect to light absorptance is determined by the absorber efficiency that changes in a significant way with temperature [13, 14], implying that the standard is not adequate to assess the performances of SSA for application different than DHW. As pointed out by Cao [10], the relative weight depends by the operating temperature and this would result in a temperature dependent PC. The use of the efficiency (eq.4) to define a performance criterion solves the problem of the PC temperature dependence and represents a more useful and appropriate criterion for absorbers working in mid-high temperature applications. The proposed performance criterion ($PC_\eta(T)$) is defined as:

$$PC_\eta(T) = \Delta\eta_{abs}(T) \tag{13}$$

with $\Delta\eta_{abs}(T) = \eta_{abs}(T) - \eta'_{abs}(T)$, where $\eta_{abs}(T)$ is the efficiency of the virgin absorber and $\eta'_{abs}(T)$ the efficiency of the absorber after test. It is worth noticing that $PC_\eta(T)$ is function of the nominal absorber temperature of operation. In fig.5c PC and $PC_\eta(T)$ are reported as function of the testing time. Both criterions have been calculated for operating temperature of 373 K, 473 K and 573 K. As expected, the two criterions are identical for 373 K operating temperature whereas differences appear at higher the operating temperature of the absorber. The difference between $PC_\eta(T)$ and PC, arises with temperature since the weight of the thermal emittance over the light absorptance increases with the temperature [10], making $PC_\eta(T)$ equal or lower than PC. The use of the proposed $PC_\eta(T)$ does not require to adjust the weighting factor of $\Delta\bar{\varepsilon}$ according to the operating temperature.

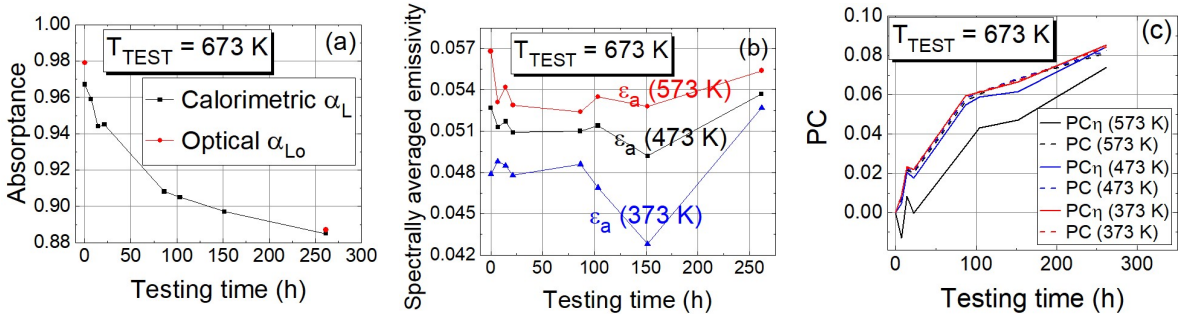

FIGURE 5. (a) Change of absorptance during test at 673 K calorimetric measurements (black squares) and optical measurements (red points). (b) Change of spectrally average emissivity at 573 K (red points), 473 K (black squares), 373 K (blue triangles) during test at 673 K calorimetric measurements. (c) Standard performance criterion ($PC = -\Delta\alpha + 0.5\Delta\bar{\varepsilon}$) and proposed performance criterion ($PC_\eta(T) = \Delta\eta_{abs}(T)$) as function of the testing time for operating temperatures of 373 K, 473 K and 573 K.

The $PC_\eta(T)$ value of end life service was established equal to 0.05 (the same of standard PC limit value) representing the maximum value of reduction of the $\eta_{abs}(T)$ during the service (25 years). The efficiency is calculated at T_{amb} = 293 K and H_{abs} = 1000 W/m^2 for a T_a = 573 K.

In table 1 the values of light absorptance, thermal emittance, absorber efficiency, $PC_\eta(T)$ and PC referred to 573 K of operating temperature are reported.

Preprints (www.preprints.org) | NOT PEER-REVIEWED | Posted: 6 July 2021 doi:10.20944/preprints202107.0128.v1

TABLE 1. Comparison, during the test, between the standard performance criterion ($PC = -\Delta\alpha + 0.5\Delta\bar{\varepsilon}$) and the proposed performance criterion ($PC_\eta(T) = \Delta\eta_{abs}(T)$) for test at 673 K.

Testing time (h)	α_L	$\bar{\varepsilon}_a$ (573 K)	η_{abs} (573 K)	η'_{abs} (573 K)	PC_η (573 K)	PC
0	0.967	0.057	0.643	-	-	-
7	0.959	0.053	-	0.656	-0.013	0.006
14	0.944	0.054	-	0.635	0.008	0.022
22	0.945	0.053	-	0.643	0.000	0.020
87	0.908	0.052	-	0.609	0.034	0.057
104	0.905	0.054	-	0.600	0.043	0.060
152	0.897	0.053	-	0.596	0.047	0.068
262	0.885	0.055	-	0.569	0.074	0.081

The maximum difference between the proposed performance criterion ($PC_\eta(T)$) and the standard one (PC) is of 0.023 at 87 h of testing time (as reported in the tab.1), while the medium difference is of 0.017. More important, the PC reaches the limit value of 0.05 after about 80 hours, when the efficiency was changed of only 0.034, whereas the proposed $PC_\eta(T)$ exceed 0.05 after more than 152 hours.

To obtain a shorter testing time, the second thermal aging test was performed at a temperature higher than 673 K. The absorber was set at 692 K and it was kept at this temperature for a total of 119.5 hours. In the fig.6a is shown the decreasing trend in absorptance, during the second test, from an initial value equal to 0.967 down to a value of 0.860, with a decrease by 10.9% absorptance. The optical measurements are in agreement with calorimetric ones showing a maximum difference of 2.8%. After 31 hours, the thermal emittance at 573 K (fig.6b) increases from 0.057 up to 0.060, whereas a slightly decrease to a value of 0.058 is observed after 119.5 hours. The proposed performance criterion was also calculated for the second test (as reported in the tab.2). The maximum difference between the proposed performance criterion ($PC_\eta(T)$) and the standard one (PC) is of 0.014 at 31 h of testing time, while the medium difference is of 0.006. In this second test the initial reduction in emittance was not observed and the $PC_\eta(T)$ values are more similar to the PC value.

Having performed two tests, E_T and D_{Arrh} can be now estimated by using data obtained from tests in eq.9 a and b (t_1= 262 hrs, T_1 = 673 K and PC^1 = 0.081 or PC_η^1 (573 K) = 0.074; t_2 = 119.5 hrs, T_2 = 692 K and PC^2 = 0.105 or PC_η^2 (573 K) = 0.110). The calculated values for these two variables are: E_T = 250 kJ/mol and D_{Arrh} = 4E+15 h^{-1} in the case of $PC_\eta(T)$ and E_T = 220 kJ/mol and D_{Arrh} = 3E+13 h^{-1} if the standard PC is used. The activation energy values obtained using the two PCs are very similar and a similar service lifetime can be expected according to eq.9.

It is worth to note the service lifetime is calculated by using eq.9 (a or b), where $T = T_{eff}$ depends by the $f(T)$. The $f(T)$ reported in the standard [17] is not adequate for applications at temperature higher than DHW. The $f(T)$ was rescaled according to the procedure describes in *M. Köhl et al.* [19] to obtain $f'(T)$ in the case of 573 K stagnation temperature and T'_{eff} was calculated according to eq.6. Thanks to these values (E_T, D_{Arrh}, T'_{eff}, PCs limit value), by means one equation of eq.9, it is possible to predict the service lifetime of the SSA under test: it results longer than 25 years also in the case of operating temperature higher than DHW for both PCs (about 500 and 1500 years for PC and PC_η respectively). It is worth to mention that, even if such estimations are obtained using LED lamps that have a spectrum different from the Sun, the result applies also to Sun illumination since the absorptances calculated using the Sun and the LED spectrum are very similar.

Preprints (www.preprints.org) | NOT PEER-REVIEWED | Posted: 6 July 2021 doi:10.20944/preprints202107.0128.v1

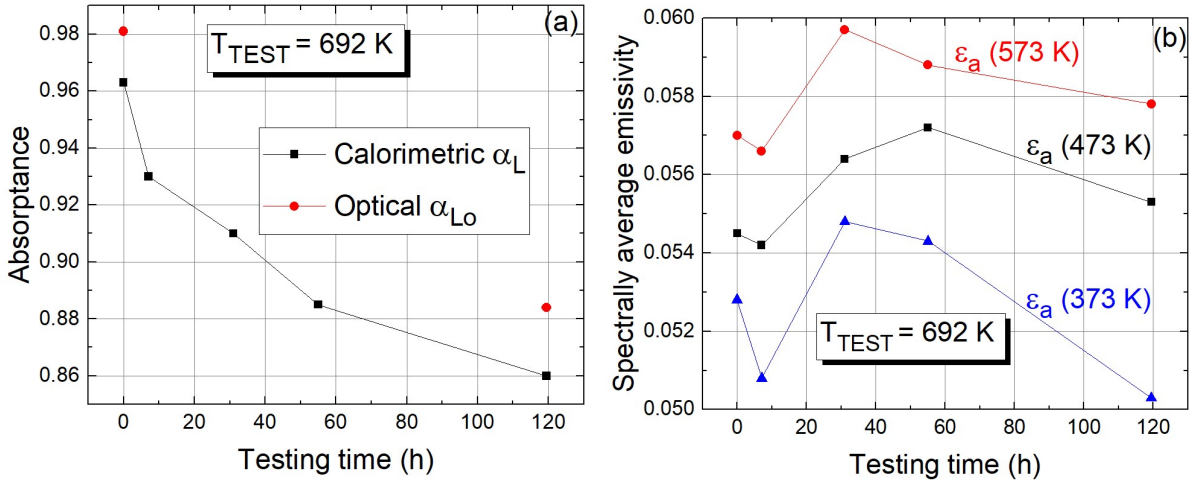

FIGURE 6. (a) Change of absorptance during test at 692 K calorimetric measurements (black squares) and optical measurements (red points). (b) Change of spectral average emissivity at 573 K (red points), 473 K (black squares), 373 K (blue triangles) during test at 692 K calorimetric measurements.

TABLE 2. Comparison, during the test, between the standard performance criterion ($PC = -\Delta\alpha + 0.5\Delta\bar{\varepsilon}$) and the proposed performance criterion ($PC_\eta(T) = \Delta\eta_{abs}(T)$) for test at 692 K.

Testing time (h)	α_L	$\bar{\varepsilon}_a$ (573 K)	η_{abs} (573 K)	η'_{abs} (573 K)	PC_η (573 K)	PC
0	0.965	0.057	0.640	-	-	-
7	0.93	0.057	-	0.607	0.033	0.035
31	0.91	0.060	-	0.570	0.070	0.056
55	0.885	0.059	-	0.550	0.090	0.081
119.5	0.86	0.058	-	0.531	0.110	0.105

5. Conclusions

In this work, a Cr based solar selective absorber designed to work at 573 K has been characterize by measurement of optical properties at working conditions and by thermal aging tests in vacuum. The measurements, obtained by means of the customized system (MTB), showed high absorptance (0.965) and low thermal emittance (0.057) at working temperature (573 K), corresponding to absorber efficiency of 0.640. Such efficiency is very close to the collector efficiency since the high vacuum in flat plate collectors reduces the convective losses to a negligible level.

In order to estimate the activation energy and the absorber lifetime service, two thermal aging tests were performed at two temperatures (673 K and 692 K). A different performance criterion ($PC_\eta(T)$) has been proposed for assessing the service lifetime at temperature high than the DHW applications. It is defined as the efficiency difference between the virgin absorber and the absorber after the ageing test. The proposed criterion has the advantage to reduce to the current used criterion for temperatures close to DHW, whereas adjusting the relative weight of absorptance and emittance as function of the operating temperature. The thermal aging tests in vacuum showed a good thermal stability of the SSA working at high temperature.

The activation energy of the aging process calculated with $PC_\eta(T)$ and standard PC is equal to 250 kJ/mol and 220 kJ/mol, respectively. The tested absorber is a good candidate for unconcentrated solar thermal applications, thanks to its good stability in vacuum at high temperatures and its long service lifetime (> 25 years).

Acknowledgments

The authors are grateful to Rosario Iameo for his help in programming the data acquisition and control software of the MTB system.

The Ph.D. grants of D.D.L. and A.C. are funded by the PON2014-2020 “Dottorati innovativi con caratterizzazione industriale” program (XXXIV ciclo and XXXV ciclo respectively). The Ph.D. grants of D.D.M. and E.G. are funded by the CNR-Confindustria “Dottorati di Ricerca Industriali” program XXXIV and XXXVI ciclo.

References

[1] A. Azam, A. Ahmed, H. Wang, Y. Wang, and Z. Zhang, ‘Knowledge structure and research progress in wind power generation (WPG) from 2005 to 2020 using CiteSpace based scientometric analysis’, *Journal of Cleaner Production*, vol. 295, p. 126496, 2021, doi: 10.1016/j.jclepro.2021.126496.

[2] I. Kougias *et al.*, ‘Analysis of emerging technologies in the hydropower sector’, *Renewable and Sustainable Energy Reviews*, vol. 113, no. July, p. 109257, Oct. 2019, doi: 10.1016/j.rser.2019.109257.

[3] G. Li, S. Shittu, T. M. O. Diallo, M. Yu, X. Zhao, and J. Ji, ‘A review of solar photovoltaic-thermoelectric hybrid system for electricity generation’, *Energy*, vol. 158, pp. 41–58, Sep. 2018, doi: 10.1016/j.energy.2018.06.021.

[4] M. Soltani *et al.*, ‘Environmental, economic, and social impacts of geothermal energy systems’, *Renewable and Sustainable Energy Reviews*, vol. 140, no. February, p. 110750, Apr. 2021, doi: 10.1016/j.rser.2021.110750.

[5] M. M. Gul and K. S. Ahmad, ‘Bioelectrochemical systems: Sustainable bio-energy powerhouses’, *Biosensors and Bioelectronics*, vol. 142, no. July, p. 111576, Oct. 2019, doi: 10.1016/j.bios.2019.111576.

[6] L. Kumar, M. Hasanuzzaman, and N. A. Rahim, ‘Global advancement of solar thermal energy technologies for industrial process heat and its future prospects: A review’, *Energy Conversion and Management*, vol. 195, no. May, pp. 885–908, Sep. 2019, doi: 10.1016/j.enconman.2019.05.081.

[7] E. Vengadesan and R. Senthil, ‘A review on recent developments in thermal performance enhancement methods of flat plate solar air collector’, *Renewable and Sustainable Energy Reviews*, vol. 134, no. November 2019, p. 110315, Dec. 2020, doi: 10.1016/j.rser.2020.110315.

[8] V. Pranesh, R. Velraj, S. Christopher, and V. Kumaresan, ‘A 50 year review of basic and applied research in compound parabolic concentrating solar thermal collector for domestic and industrial applications’, *Solar Energy*, vol. 187, no. April, pp. 293–340, Jul. 2019, doi: 10.1016/j.solener.2019.04.056.

[9] A. Buonomano *et al.*, ‘Experimental analysis and dynamic simulation of a novel high-temperature solar cooling system’, *Energy Conversion and Management*, vol. 109, pp. 19–39, Feb. 2016, doi: 10.1016/j.enconman.2015.11.047.

[10] F. Cao, K. McEnaney, G. Chen, and Z. Ren, ‘A review of cermet-based spectrally selective solar absorbers’, *Energy & Environmental Science*, vol. 7, no. 5, p. 1615, 2014, doi: 10.1039/c3ee43825b.

[11] O. Raccurt and A. Disdier, ‘Accelerated ageing tests for durability study of solar absorber coatings on metallic substrate for solar thermal energy (STE) application’, in *AIP Conference Proceedings 2033*, 2018, vol. 230011, p. 230011. doi: 10.1063/1.5067239.

[12] O. Raccurt, A. Disdier, D. Bourdon, S. Donnola, A. Stollo, and A. Gioconia, ‘Study of the Stability of a Selective Solar Absorber Coating under Air and High Temperature Conditions’, *Energy Procedia*, vol. 69, no. 0, pp. 1551–1557, May 2015, doi: 10.1016/j.egypro.2015.03.107.

[13] D. De Maio *et al.*, ‘A Selective Solar Absorber for Unconcentrated Solar Thermal Panels’, *Energies*, no. 2, 2021, doi: https://doi.org/10.3390/ en14040900.

[14] R. Russo, M. Monti, F. di Giamberardino, and V. G. Palmieri, ‘Characterization of selective solar absorber under high vacuum’, *Optics Express*, vol. 26, no. 10, p. A480, May 2018, doi: 10.1364/OE.26.00A480.

[15] C. D'Alessandro *et al.*, 'Low cost high intensity LED illumination device for high uniformity solar testing', *Solar Energy*, vol. 221, pp. 140–147, Jun. 2021, doi: 10.1016/j.solener.2021.04.017.

[16] R. Russo *et al.*, 'The Absorptance of Selective Solar Absorber Working in High Vacuum', in *20th Italian National Conference on Photonic Technologies (Fotonica 2018)*, Lecce, Italy, 2018, p. 56 (4 pp.)-56 (4 pp.). doi: 10.1049/cp.2018.1665.

[17] B. Carlsson, K. Moeller, U. Frei, and M. Koehl, 'Accelerated life testing of solar absorber coatings', Sep. 1994, pp. 79–90. doi: 10.1117/12.185359.

[18] C. D'Alessandro *et al.*, 'Multilayers for efficient thermal energy conversion in high vacuum flat solar thermal panels', *Submitted to the same special issue*, 2021.

[19] M. Köhl, M. Heck, S. Brunold, U. Frei, B. Carlsson, and K. Möller, 'Advanced procedure for the assessment of the lifetime of solar absorber coatings', *Solar Energy Materials and Solar Cells*, vol. 84, no. 1–4, pp. 275–289, Oct. 2004, doi: 10.1016/j.solmat.2004.01.041.

Preprints (www.preprints.org) | NOT PEER-REVIEWED | Posted: 6 July 2021 doi:10.20944/preprints202107.0128.v1

Figure captions:

1. Ideal absorber spectral emissivity designed for 573 K (black dashed line), blackbody emission E_{BB} at 573 K (black line) and Solar Spectrum (orange line).
2. The mini test box system with LED array system.
3. a) Spectral averaged emissivity ($\bar{\varepsilon}_{tot}(T_a)$) calculated by means MTB system (black line) and fitted (red line) b) Left axis: spectrum on the LED Array used to illuminate the absorber. Right axis: absorptivity measured with integrating sphere and an Optical spectrum analyser at room temperature.
4. (a) Spectral averaged emissivity calculated by means MTB system for copper (black line) and fitted (red line). (b) The thermal emittance as function of temperature of: the whole sample ($\bar{\varepsilon}_{tot}(T_a)$ black line), the copper substrate ($\bar{\varepsilon}_{sub}(T_{sub})$ blue dashed line), and the SSA under test ($\bar{\varepsilon}_a(T_a)$ thick red line).
5. (a) Change of absorptance during test at 673 K calorimetric measurements (black squares) and optical measurements (red points). (b) Change of spectrally average emissivity at 573 K (red points), 473 K (black squares), 373 K (blue triangles) during test at 673 K calorimetric measurements. (c) Standard performance criterion ($PC = -\Delta\alpha + 0.5\Delta\bar{\varepsilon}$) and proposed performance criterion ($PC_\eta(T) = \Delta\eta_{abs}(T)$) as function of the testing time for operating temperatures of 373 K, 473 K and 573 K.
6. (a) Change of absorptance during test at 692 K calorimetric measurements (black squares) and optical measurements (red points). (b) Change of spectral average emissivity at 573 K (red points), 473 K (black squares), 373 K (blue triangles) during test at 692 K calorimetric measurements.

Preprints (www.preprints.org) | NOT PEER-REVIEWED | Posted: 6 July 2021 doi:10.20944/preprints202107.0128.v1

Table captions:

1. Comparison, during the test, between the standard performance criterion ($PC = -\Delta\alpha + 0.5\Delta\bar{\varepsilon}$) and the proposed performance criterion ($PC_\eta(T) = \Delta\eta_{abs}(T)$) for test at 673 K.
2. Comparison, during the test, between the standard performance criterion ($\mathrm{PC} = -\Delta\alpha + 0.5\Delta\bar{\varepsilon}$) and the proposed performance criterion ($\mathrm{PC}_\eta(\mathrm{T}) = \Delta\eta_{\mathrm{abs}}(\mathrm{T})$) for test at 692 K.